

Basic Study

Signal transducer and activator of transcription 3 promotes the Warburg effect possibly by inducing pyruvate kinase M2 phosphorylation in liver precancerous lesions

Yang-Hui Bi, Wen-Qi Han, Ruo-Fei Li, Yun-Jiao Wang, Zun-Shu Du, Xue-Jiang Wang, Ying Jiang

ORCID number: Yang-Hui Bi (0000-0002-3039-6072); Wen-Qi Han (0000-0003-3106-4210); Ruo-Fei Li (0000-0001-6733-1486); Yun-Jiao Wang (0000-0002-1778-5735); Zun-Shu Du (0000-0002-1516-816X); Xue-Jiang Wang (0000-0003-4772-7365); Ying Jiang (0000-0001-5908-0904).

Author contributions: Bi YH and Han WQ contributed equally to this work; Jiang Y and Wang XJ designed the research; Jiang Y, Bi YH, Han WQ, Li RF, Wang XJ, and Du ZS performed the research; Jiang Y contributed new reagents or analytic tools; Jiang Y, Bi YH, and Han WQ analyzed the data and wrote the paper; all of the authors have read and approved the final manuscript.

Supported by the National Natural Science Foundation of China, No. 81070319; the Beijing Natural Science Foundation of China, No. 7102013; and the Beijing Municipal Education Commission Research Program, China, No. KM201610025004.

Institutional animal care and use committee statement: All procedures involving animals were reviewed and approved by the Institutional Animal Care and Use Committee of the Capital Medical University [IACUC protocol number: (AEEL-2016-118)].

Conflict-of-interest statement: The authors have no conflicts of interest to declare.

Data sharing statement: The

Yang-Hui Bi, Wen-Qi Han, Ruo-Fei Li, Yun-Jiao Wang, Zun-Shu Du, Xue-Jiang Wang, Ying Jiang, Department of Physiology and Pathophysiology, School of Basic Medical Sciences, Capital Medical University, Beijing 100069, China

Corresponding author: Ying Jiang, PhD, Professor, Department of Physiology and Pathophysiology, School of Basic Medical Sciences, Capital Medical University, No. 10, Xitoutiao, You An Men Wai, Beijing 100069, China. jiangy@ccmu.edu.cn
Telephone: +86-10-83911687

Abstract**BACKGROUND**

Study shows that signal transducer and activator of transcription 3 (STAT3) can increase the Warburg effect by stimulating hexokinase 2 in breast cancer and upregulate lactate dehydrogenase A and pyruvate dehydrogenase kinase 1 in myeloma. STAT3 and pyruvate kinase M2 (PKM2) can also be activated and enhance the Warburg effect in hepatocellular carcinoma. Precancerous lesions are critical to human and rodent hepatocarcinogenesis. However, the underlying molecular mechanism for the development of liver precancerous lesions remains unknown. We hypothesized that STAT3 promotes the Warburg effect possibly by upregulating p-PKM2 in liver precancerous lesions in rats.

AIM

To investigate the mechanism of the Warburg effect in liver precancerous lesions in rats.

METHODS

A model of liver precancerous lesions was established by a modified Solt-Farber method. The liver pathological changes were observed by HE staining and immunohistochemistry. The transformation of WB-F344 cells induced with N-methyl-N'-nitro-N-nitrosoguanidine and hydrogen peroxide was evaluated by the soft agar assay and aneuploidy. The levels of glucose and lactate in the tissue and culture medium were detected with a spectrophotometer. The protein levels of glutathione S-transferase-II, proliferating cell nuclear antigen (PCNA), STAT3, and PKM2 were examined by Western blot and immunofluorescence.

RESULTS

We found that the Warburg effect was increased in liver precancerous lesions in rats. PKM2 and p-STAT3 were upregulated in activated oval cells in liver

manuscript has no additional data available.

ARRIVE guidelines statement: The authors have read the ARRIVE guidelines, and the manuscript was prepared and revised according to the ARRIVE guidelines.

Open-Access: This article is an open-access article which was selected by an in-house editor and fully peer-reviewed by external reviewers. It is distributed in accordance with the Creative Commons Attribution Non Commercial (CC BY-NC 4.0) license, which permits others to distribute, remix, adapt, build upon this work non-commercially, and license their derivative works on different terms, provided the original work is properly cited and the use is non-commercial. See: <http://creativecommons.org/licenses/by-nc/4.0/>

Manuscript source: Unsolicited manuscript

Received: January 27, 2019

Peer-review started: January 27, 2019

First decision: February 26, 2019

Revised: March 7, 2019

Accepted: March 24, 2019

Article in press: March 25, 2019

Published online: April 28, 2019

P-Reviewer: Baddour N, Lu WY

S-Editor: Ma RY

L-Editor: Wang TQ

E-Editor: Song H



precancerous lesions in rats. The Warburg effect, p-PKM2, and p-STAT3 expression were also increased in transformed WB-F344 cells. STAT3 activation promoted the clonal formation rate, aneuploidy, alpha-fetoprotein expression, PCNA expression, G1/S phase transition, the Warburg effect, PKM2 phosphorylation, and nuclear translocation in transformed WB-F344 cells. Moreover, the Warburg effect was inhibited by stattic, a specific inhibitor of STAT3, and further reduced in transformed WB-F344 cells after the intervention for PKM2.

CONCLUSION

The Warburg effect is initiated in liver precancerous lesions in rats. STAT3 activation promotes the Warburg effect by enhancing the phosphorylation of PKM2 in transformed WB-F344 cells.

Key words: Warburg effect; Hepatic progenitor cell; Signal transducer and activator of transcription 3; Pyruvate kinase M2; Liver precancerous lesion

©The Author(s) 2019. Published by Baishideng Publishing Group Inc. All rights reserved.

Core tip: Signal transducer and activator of transcription 3 (STAT3) is stimulated in hepatocellular carcinoma and regulates the Warburg effect in many tumors. However, whether the activation of STAT3 can enhance the Warburg effect is unclear in liver precancerous lesions. Here, we provide the evidence that the Warburg effect was enhanced in liver precancerous lesions in rats, perhaps through up-regulating the expression of pyruvate kinase M2 (PKM2) and p-STAT3 in activated oval cells. STAT3 activation promotes the Warburg effect by activating PKM2 in transformed WB-F344 cells induced with N-methyl-N²-nitro-N-nitrosoguanidine and hydrogen peroxide.

Citation: Bi YH, Han WQ, Li RF, Wang YJ, Du ZS, Wang XJ, Jiang Y. Signal transducer and activator of transcription 3 promotes the Warburg effect possibly by inducing pyruvate kinase M2 phosphorylation in liver precancerous lesions. *World J Gastroenterol* 2019; 25(16): 1936-1949

URL: <https://www.wjgnet.com/1007-9327/full/v25/i16/1936.htm>

DOI: <https://dx.doi.org/10.3748/wjg.v25.i16.1936>

INTRODUCTION

Cancerous cells transform significant amounts of glucose into lactate irrespective of oxygen availability. This phenomenon, also known as aerobic glycolysis or the Warburg effect, meets the energetic demands of tumor cells and provides them with growth and survival advantages. The Warburg effect is frequently enhanced in hepatocellular carcinoma (HCC)^[1,2]. Many studies have shown that HCC is closely associated with precancerous lesions. Liver precancerous lesions are well-established histopathologically premalignant tissue with the highest risk for tumorigenesis and are critical for hepatocarcinogenesis in human and rodents^[3-5]. Recognition and treatment at the precancerous stage might reduce the incidence and mortality of HCC. However, the underlying molecular mechanism for the development of liver precancerous lesions remains unclear.

The liver stem cell differentiation arrest theory and the dedifferentiation of mature hepatocytes theory are two widely accepted hypotheses of hepatocarcinogenesis. Studies have noted a progenitor cell phenotype in many HCCs. Alterations in the hepatic niche can lead to the malignant transformation of hepatic progenitor cells^[6-8]. Signal transducer and activator of transcription 3 (STAT3) is a member of the STAT family of transcription factors and is activated in several cancers with a poor prognosis, such as HCC, breast cancer, and esophageal squamous cell carcinoma^[9-11]. Once it is activated by tyrosine phosphorylation, STAT3 translocates into the nucleus and regulates the expression of target genes, mediating numerous aspects of tumorigenesis, including proliferation, angiogenesis, immunity, motility, apoptosis, and cell differentiation^[12,13]. In addition, STAT3 can regulate aerobic glycolysis in breast cancer cells by stimulating the transcription of hexokinase 2^[14]. STAT3 also upregulates lactate dehydrogenase A and pyruvate dehydrogenase kinase 1 to

increase glycolysis in myeloma cells^[15]. However, whether activation of STAT3 enhances the Warburg effect in liver precancerous lesions and the underlying mechanism remain unclear.

Pyruvate kinase (PK), a key enzyme in glycolysis, catalyzes the synthesis of pyruvate and ATP, using phosphoenolpyruvate (PEP) and ADP as substrates. There are four mammalian pyruvate kinase isoforms: PKL, PKR, PKM1, and PKM2. PKL is mainly expressed in the liver and kidney, and PKR is highly expressed in erythrocytes. PKM1 is preferentially expressed in adult tissues, while PKM2 is abundantly expressed in rapidly proliferating tissues, embryos, and tumors^[16-18]. Recent studies have shown that PKM1 can promote tumor cell proliferation and activate glucose catabolism in small-cell lung cancer (SCLC)^[19]. But more results confirm that among the four mammalian pyruvate kinase isoforms, PKM2 is most closely related to tumor cell proliferation. PKM2 is an important regulator of the Warburg effect and is highly expressed in many tumors. Tetrameric PKM2 has PK activity in normal cells. PKM2 tetramers are tyrosine-phosphorylated at Y105 to transform dimeric PKM2 in tumor cells^[20,21]. Then, PKM2 dimers promote the synthesis of deoxynucleotides, providing tumor cells with a growth and proliferation advantage. Dimeric PKM2 can enhance aerobic glycolysis, increase lactate production, and regulate the expression of genes that mediate the Warburg effect in many tumors^[18,20], including HCC^[22]. However, whether STAT3 activation enhances the phosphorylation of PKM2 in cancer is unknown.

Here, we showed that Warburg effect was initiated in liver precancerous lesions in rats and STAT3 phosphorylation was involved in liver precancerous lesions probably by activating hepatic progenitor cells in the Solt-Farber model. Furthermore, we confirm that STAT3 activation promoted the Warburg effect by upregulating p-PKM2 in transformed hepatic progenitor cells in rats. Our study can help better understand the role of STAT3 and PKM2 in HCC formation.

MATERIALS AND METHODS

Experimental animals

Sixty adult male Wistar rats (6 wk old), weighing 180-200 g, were purchased from Beijing Vital River Laboratory Animal Technology Co. Ltd (Beijing, China). All animal feeding and experimental procedures were approved by the Ethical Committee of Capital Medical University and were performed according to National Institutes of Health (NIH) Guidelines. A modified Solt-Farber model of liver precancerous lesions was generated as described^[23,24]. The animals were acclimatized to laboratory conditions (23 °C, 12 h/12 h light/dark, 50% humidity, *ad libitum* access to food and water) for 1 wk prior to experimentation. Then, a single dose of diethylnitrosamine (DEN, 200 mg/kg body weight; Sigma, St. Louis, MO, United States) was injected intraperitoneally. After a two-week recovery, the rats were subcutaneously inserted with 2-acetylaminofluorene (2-AAF; Innovative Research, Miami, FL, United States) pellets (50 mg/pellet over a 21-d release) for 1 wk followed by a two-thirds partial hepatectomy (PH). The animals were then euthanized nine days after PH. The livers of the rats were removed rapidly and dissected. Rats with no treatment, rats exposed to DEN and PH, and rats exposed to AAF and PH were used as controls.

Cell culture

The WB-F344 rat hepatic progenitor cell line (a gift from Dr. Geng-Tao Liu, Peking Union Medical College) was cultured in Dulbecco's Modified Eagle Medium and Nutrient Mixture F-12 (DMEM/F12) (Hyclone) with 100 U/mL penicillin and 100 µg/mL streptomycin with or without 10% fetal bovine serum (FBS; Corning, KS, United States). The cells were maintained in the logarithmic growth phase at 37 °C in 5% CO₂. We induced the malignant transformation of WB-F344 cells according to a previous study^[25,26]. Briefly, WB-F344 cells were exposed to 3 µg/mL N-methyl-N'-nitro-N-nitrosoguanidine (MNNG) for 24 h, and then the cells were treated with 7 × 10⁻⁷ mol/L H₂O₂ for 12 h per day for 21 d. WB-F344 cells with no treatment was cultured as controls.

Histopathology

Rat livers were fixed in formalin for 24 h, paraffin-embedded, and sectioned into 5-µm-thick slices for hematoxylin and eosin (HE) staining.

Immunohistochemistry

Immunohistochemistry was performed as previously described. Sections were incubated with rabbit anti-PKM2 (1:800; CST, MA, United States) and rabbit anti-glutathione S-transferase-π (GST-π; 1:1000; MBL, Nagoya, Japan) overnight at 4 °C.

The appropriate secondary antibody (goat anti-rabbit IgG, ZSGB-BIO, Beijing, China) was applied for 30 min, and 3,3'-diaminobenzidine was used as the chromogen. Negative controls were run for each antibody, using PBS instead of the primary antibody. Representative images were captured with an Axio Imager 2 (Zeiss, OBK, Germany).

Immunofluorescence

Immunofluorescence was conducted as described. The slices were incubated at 4 °C overnight with mouse anti-OV-6 antibody (1:150; Roche, Basel, Switzerland) and rabbit anti-PKM2 antibody (1:50; CST) or rabbit anti-p-STAT3 antibody (1:100; CST), followed by fluorescent staining with FITC-conjugated anti-mouse IgG and Alexa Fluor 594-conjugated anti-rabbit IgG (Jackson, PA, United States). DAPI was used to stain the nuclei in the tissue samples. Images were captured with an Axio Imager 2.

Soft agar assay

Cell were assessed for colony formation in soft agar assays using a Cell Biolabs Cytosolic Cell Transformation Assay kit (Cell Biolabs, CA, United States) as per manufacturer's instructions.

Analysis of glucose consumption and lactate production

Liver tissue samples were lysed in ice-cold normal saline (0.3%). Cells were seeded in 6-well plates (8.5×10^5 cells/well). The glucose and lactate concentrations in the medium and liver tissue homogenate were measured by the glucose-oxidase method (Applygen Technologies, Beijing, China) and with a lactic acid assay kit (Nanjing Jiancheng Biotechnology, Nanjing, China), separately. The glucose consumption and lactate production were normalized to protein concentration and cell numbers.

Cell cycle and aneuploidy cells assay

The cell cycle was examined by flow cytometry. Cells (10^6 cell/mL) were harvested and fixed in 75% alcohol at 4 °C overnight. After a wash step in PBS, 500 μ L of cell cycle reagent propidium iodide (PI)/RNase staining solution (CST, MA, United States) was added to each tube and incubated for 30 min at room temperature in the dark. DNA content was analyzed on an EPICS^{XL} flow cytometer (Beckman Coulter, CA, United States). DNA content of diploid cells in WB-F344 cells was used as an internal standard to determine DNA index (DI). Cells with a DI = 0.95-1.05 were defined as diploid, cells with a DI = 1.92-2.04 were defined as tetraploid, and cells with a DI > 2.04 was considered as aneuploid^[27]. Three independent experiments were performed for each assay condition.

Cellular ATP level

Cells were seeded in 96-well plates (5×10^4 cells/well). At the end of the treatments, the cell resuspension solution was collected. ATP content was measured using the CellTiter-Glo2.0 assay kit (Promega, WI, United States) and normalized to cell numbers. Three independent experiments were performed for each assay condition.

Western blot analysis

Liver tissue samples were lysed in ice-cold RIPA buffer that was supplemented with protease inhibitors. Protein concentrations were determined using a bicinchoninic acid protein assay kit (Thermo, MA, United States). The protein extracts from liver tissue (50-100 μ g) and cell lysates (40-60 μ g) were separated by 10% sodium dodecyl sulfate-polyacrylamide gel electrophoresis and transferred to polyvinylidene difluoride membranes (Millipore, MA, United States) for Western blot analysis. The membranes were incubated with primary antibodies at 4 °C overnight and then were incubated with the appropriate secondary antibodies at room temperature. The primary antibodies included antibodies against GST- π (MBL, Nagoya, Japan), alpha-fetoprotein (AFP; Proteintech, Chicago, United States), GAPDH (GXY, Beijing, China), cytokeratin 19 (CK19), PKM2, p-PKM2, STAT3, p-STAT3, proliferating cell nuclear antigen (PCNA), β -tubulin, and β -actin (CST, MA, United States). The protein bands were visualized using enhanced chemiluminescence detection reagents (Applygen, Beijing, China) and scanned on a FlourChem HD2 System (Protein Simple, CA, United States).

Cell transfection with siRNA

Cells were seeded into 6-well plates (1.0×10^5 cells/well) on the day before the transfection. The siRNA for PKM2 (Invitrogen, Carlsbad, CA, United States) was used for the transfection of the cells, which was achieved by using LipofectamineTM RNAiMAX (Invitrogen, Carlsbad, CA, United States), according to the manufacturer's lipofection protocol. The sequence of siRNA for PKM2 was 5'-GCAGCUUUG

AUAGUUCUGATT-3'. The nonspecific miRNA (Invitrogen, Carlsbad, CA, United States) was used as a control for nonspecific effects. The effects manifested after the introduction of the mature siRNA into the cells were assayed at 72 h after the transfection.

Statistical analysis

Data are expressed as the mean \pm SEM. Statistical significance was determined by one-way ANOVA using SPSS 17.0 (SPSS, Chicago, IL, United States). $P < 0.05$ was considered statistically significant.

RESULTS

p-STAT3 participates in the formation of liver precancerous lesions in rats by activating hepatic progenitor cells

By HE staining, many heterocellular clusters in the liver parenchyma and portal area were observed in Solt-Farber model rats, the cells in the heterocellular clusters were characterized by deep nuclear staining, nuclear atypia, large karyoplasmic ratio, disordered arrangement of hepatocyte cords, and inflammatory cell infiltration. Compared with the model group, heterocellular clusters were hardly observed in the DEN + PH or normal group. In addition, significant proliferation of hepatic oval cells was observed in the liver tissues of rats both in the model group and AAF + PH group (Figure 1A). By immunohistochemistry, GST- π , a neoplastic marker in the early stages of carcinogenesis in HCC^[28], was clearly stained in the heterocellular clusters in the model group (Figure 1B). In contrast, GST- π was hardly expressed in the DEN + PH, AAF + PH, or normal group, except in the portal area (Figure 1B). This result was also shown by Western blot (Figure 1C). Oval cell 6 (OV6) and cytokeratin 19 (CK19) are molecular markers of hepatic progenitor cells in rats. By immunofluorescence, OV6 was strongly expressed in the heterocellular clusters in the model group (Figure 1D), consistent with the studies of Solt and Dunsford^[23,29]. Western blot analysis also showed that the expression of CK19 in the model group was elevated (Figure 1F)^[30]. These results suggest that the hepatic progenitor cells are activated in liver precancerous lesions in rats. Then, we further evaluated p-STAT3 expression in liver precancerous lesions. The expression of p-STAT3 in the model group was significantly higher than that in the DEN + PH, AAF + PH, and normal groups (Figure 1D and E). Notably, OV6 and p-STAT3 were co-expressed in the same heterocellular clusters (Figure 1D). These results suggest that the activation of STAT3 is closely related to the activation of hepatic progenitor cells in the progression of liver precancerous lesions in rats.

The Warburg effect is increased in liver precancerous lesions in rats, and PKM2 in activated hepatic progenitor cells is associated with liver precancerous lesions

We detected glucose and lactate concentrations in liver tissue to determine whether the Warburg effect was initiated at the stage of liver precancerous lesions. The residual concentration of glucose in the model group was markedly decreased (Figure 2A). Likewise, the concentration of lactate in the model group was elevated (Figure 2B). These results illustrate that the Warburg effect has been initiated at the stage of the liver precancerous lesions in rats.

PKM2 plays a vital role in the Warburg effect of tumors^[31]. We detected the expression of PKM2 in liver precancerous lesions. The result showed that the expression of PKM2 in the model group was significantly higher than that in the DEN + PH, AAF + PH, or normal group, and there were a large number of PKM2-positive cells around the portal area in the model group (Figure 2C and D). Especially, PKM2 was elevated in activated hepatic progenitor cells in the model group (Figure 2E). These results suggest that PKM2 is involved in the progression of activated hepatic progenitor cells in the liver precancerous lesions in rats.

p-STAT3 promotes malignant transformation of rat hepatic progenitor cells by enhancing cell proliferation

In order to explore the mechanism of STAT3 involvement in liver precancerous lesions, we replicated a model of transformed hepatic progenitor cells *in vitro* using MNNG and H₂O₂ in light of previous findings^[25,26]. Transformed WB-F344 cells became anomalous and changed in size, and contact inhibition disappeared compared with wild WB-F344 cells. The rate of aneuploidy in transformed WB-F344 cells increased to 24% compared with wild-type WB-F344 cells (Figure 3A). Furthermore, the results of soft agar assay showed that clonal formation rate of transformed WB-F344 cells was increased compared with the control group (Figure 3B). This indicates

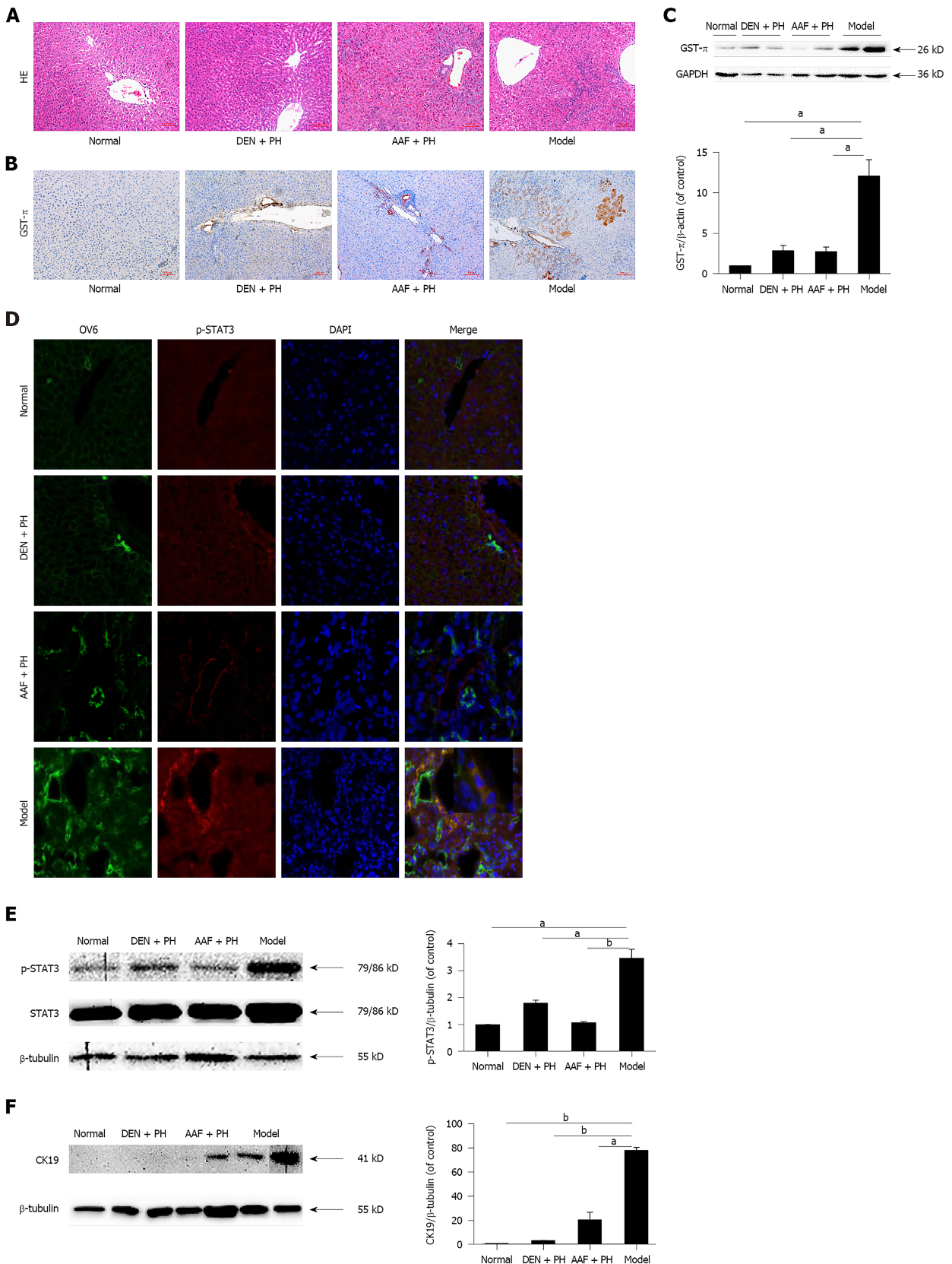


Figure 1 Pathological changes in liver precancerous lesions in rats. **A:** Heterocellular clusters were observed in the model group by hematoxylin and eosin staining. Scale bars: 100 μ m. **B and C:** Glutathione S-transferase- π was highly expressed in the model group, as revealed by immunohistochemistry and Western blot. Scale bars: 100 μ m. **D:** Immunofluorescence images showing that p-signal transducer and activator of transcription 3 (STAT3) was highly expressed in activated oval cells in the model group compared with the diethylnitrosamine (DEN) + partial hepatectomy (PH), acetylaminofluorene (AAF) + PH, and normal groups. Scale bars: 50 μ m. **E:** Western blot analysis showed that p-STAT3 was highly expressed in the model group compared with the DEN + PH, AAF + PH, and normal groups. **F:** Western blot analysis showed that cyokeratin 19 was highly expressed in the model group compared with the DEN + PH, AAF + PH, and normal groups. All values are the mean \pm SEM derived from three independent experiments (^a $P < 0.05$, ^b $P < 0.01$). GST- π : Glutathione S-transferase- π ; STAT3: Signal transducer and activator of transcription 3; CK19: Cyokeratin 19; DEN: Diethylnitrosamine; PH: Partial hepatectomy; AAF: Acetylaminofluorene; HE: Hematoxylin and eosin; OV6: Oval cell 6.

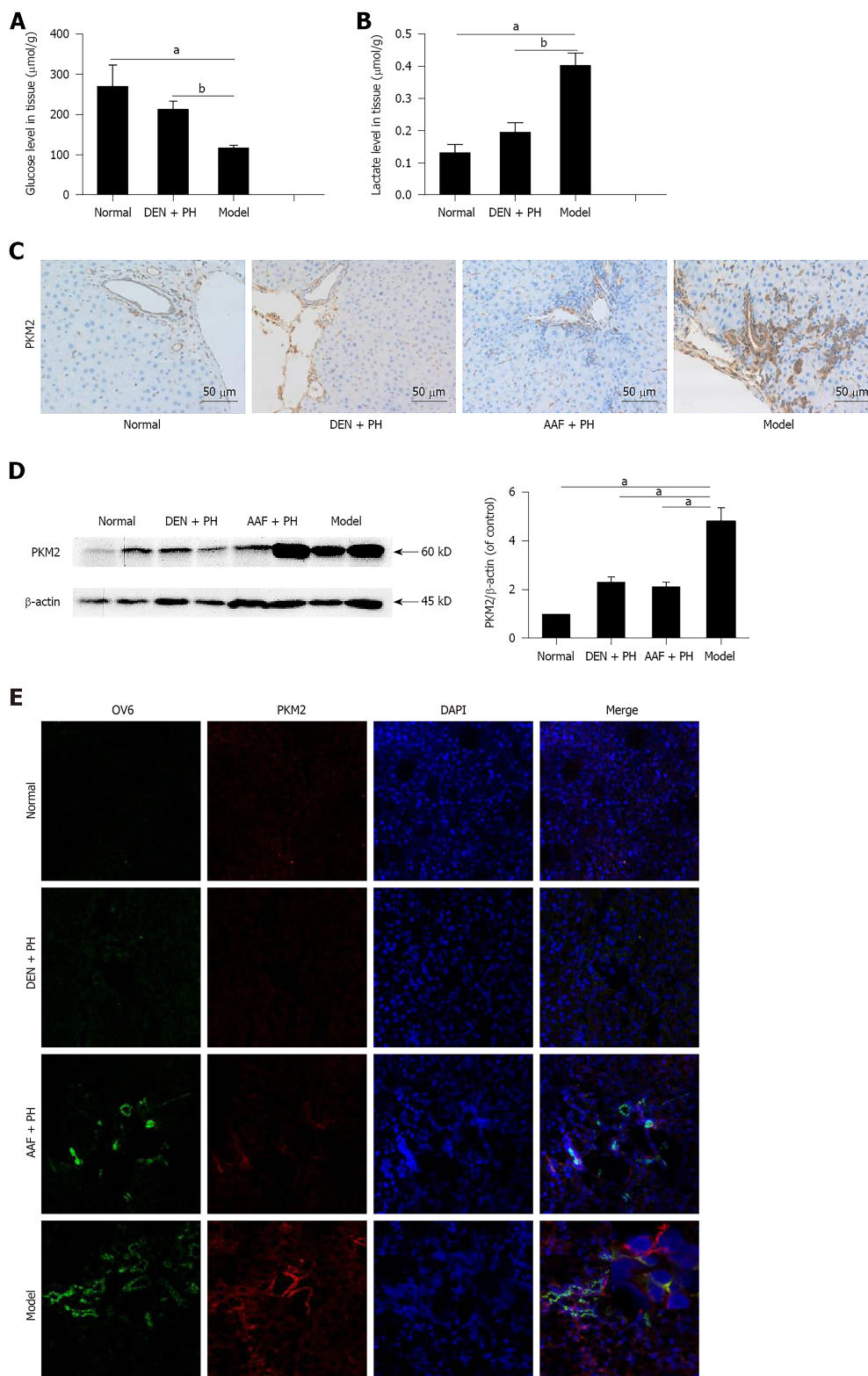


Figure 2 The Warburg effect is initiated in liver precancerous lesions in rats. A and B: The glucose consumption and lactate production in the model group were elevated compared with those in the diethylnitrosamine (DEN) + partial hepatectomy (PH) and normal groups. C and D: Immunohistochemistry and Western blot analysis showed that pyruvate kinase M2 (PKM2) was highly expressed in the model group compared with that in the DEN + PH, acetylaminofluorene (AAF) + PH, and normal groups. Scale bars: 50 µm. All values are the mean ± SEM derived from three independent experiments (^a*P* < 0.05, ^b*P* < 0.01). E: Immunofluorescence images showing that PKM2 was highly expressed in activated oval cells in the model group compared with the DEN + PH, AAF + PH, and normal groups. Scale bars: 75 µm. PKM2: Pyruvate kinase M2; DEN: Diethylnitrosamine; PH: Partial hepatectomy; AAF: Acetylaminofluorene; OV6: Oval cell 6.

that the transformed cells had the characteristics of anchorage-independent growth, which is considered the most accurate and stringent *in vitro* assay for detecting malignant transformation of cells. AFP expression further supported the conclusion above (Figure 3C). These results suggest that the WB-F344 cells induced with MNNG

and H₂O₂ gained the characteristics of transformed cells.

In addition, p-STAT3 expression in transformed WB-F344 cells was higher than that in wild-type WB-F344 cells (Figure 3D). Next, we used stattic (MedChem Express, Monmouth Junction, NJ, United States), a specific inhibitor of STAT3, to suppress the activation of STAT3 in transformed hepatic progenitor cells. Compared with transformed WB-F344 cells, p-STAT3, aneuploidy, the clonal formation rate, and AFP expression decreased following 4 μmol/L stattic treatment (results of cell viability are not shown) (Figure 3A-D). These results indicate that STAT3 promotes malignant transformation of hepatic progenitor cells in rats.

To determine the mechanism by which STAT3 promotes malignant transformation of hepatic progenitor cells in rats, we measured PCNA expression and the cell cycle in transformed WB-F344 cells. As shown in Figure 3E, PCNA was highly expressed in transformed WB-F344 cells compared with wild-type WB-F344 cells, and PCNA was inhibited following stattic treatment. The percentage of transformed WB-F344 cells in S phase was increased compared with wild-type WB-F344 cells. STAT3 inhibition by stattic also significantly mitigated the increase in transformed WB-F344 cells in S phase (Figure 3F). These results suggest that STAT3 promotes malignant transformation of hepatic progenitor cells by enhancing cell proliferation.

STAT3 promotes the Warburg effect by enhancing p-PKM2 in transformed hepatic progenitor cells in rats

As shown in Figure 4A, transformed WB-F344 cells took up much higher amounts of glucose than wild-type WB-F344 cells. Similarly, lactate production in transformed WB-F344 cells was higher than that in wild-type WB-F344 cells (Figure 4B). These results suggest that the Warburg effect was initiated in transformed hepatic progenitor cells. The production of ATP in transformed WB-F344 cells was steady compared with wild-type WB-F344 cells (Figure 4C), in accordance with a previous study^[32]. In addition, in order to investigate the effect of PKM2 on the Warburg effect in transformed hepatic progenitor cells, we also measured the expression of p-PKM2. By Western blot analysis, it was discovered that the expression of p-PKM2 in transformed WB-F344 cells was significantly higher than that in wild-type WB-F344 cells (Figure 4D). The same results were obtained by immunofluorescence assay, and the expression of PKM2 in the nucleus was significantly increased in transformed WB-F344 cells (Figure 4E).

To determine the function and mechanism of STAT3 in the Warburg effect in transformed hepatic progenitor cells, we measured the influence of stattic treatment on the Warburg effect. The consumption of glucose, the production of lactate, and ATP levels were decreased following STAT3 inhibition by stattic (Figure 4A-C). These results indicate that STAT3 promotes the Warburg effect in transformed hepatic progenitor cells. And after STAT3 inhibition by stattic, p-PKM2 expression and nuclear translocation were also decreased (Figure 4D and E). These results indicate that STAT3 promotes the PKM2 expression and nuclear translocation in transformed hepatic progenitor cells.

To explore whether STAT3 works through PKM2, TEPP-46 (MedChem Express, Monmouth Junction, NJ, United States), a potent and selective activator of PKM2 that promotes the formation of PKM2 tetramers, was used to act on the malignant transformed WB-F344 cells after stattic treatment^[33]. The results showed that the suppressed Warburg effect by stattic was further reduced in transformed WB-F344 cells. Further use of PKM2 siRNA also resulted in the similar phenomenon (Figure 4A-C). These results suggest that STAT3 promotes the Warburg effect in transformed hepatic progenitor cells probably by upregulating p-PKM2.

DISCUSSION

Recent studies have shown that STAT3 plays a vital role in the Warburg effect and adjusts the activity of key enzymes in the glycolytic pathway in tumor cells^[34]. STAT3 regulates aerobic glycolysis in breast cancer cells by stimulating hexokinase 2 transcription^[14]. STAT3 also increased glycolysis in myeloma cells by upregulating lactate dehydrogenase A and pyruvate dehydrogenase kinase 1^[15]. However, little work has been performed to determine the mechanism of STAT3 in promoting the Warburg effect in hepatocarcinogenesis. In our study, we observed that the Warburg effect was initiated at the stage of liver precancerous lesions, likely through activation of STAT3 and PKM2, in the Solt-Farber model. What's more, STAT3 promoted the Warburg effect possibly by enhancing p-PKM2 in transformed hepatic progenitor cells in rats.

The theory of dedifferentiation of mature hepatocytes and the theory of abnormal

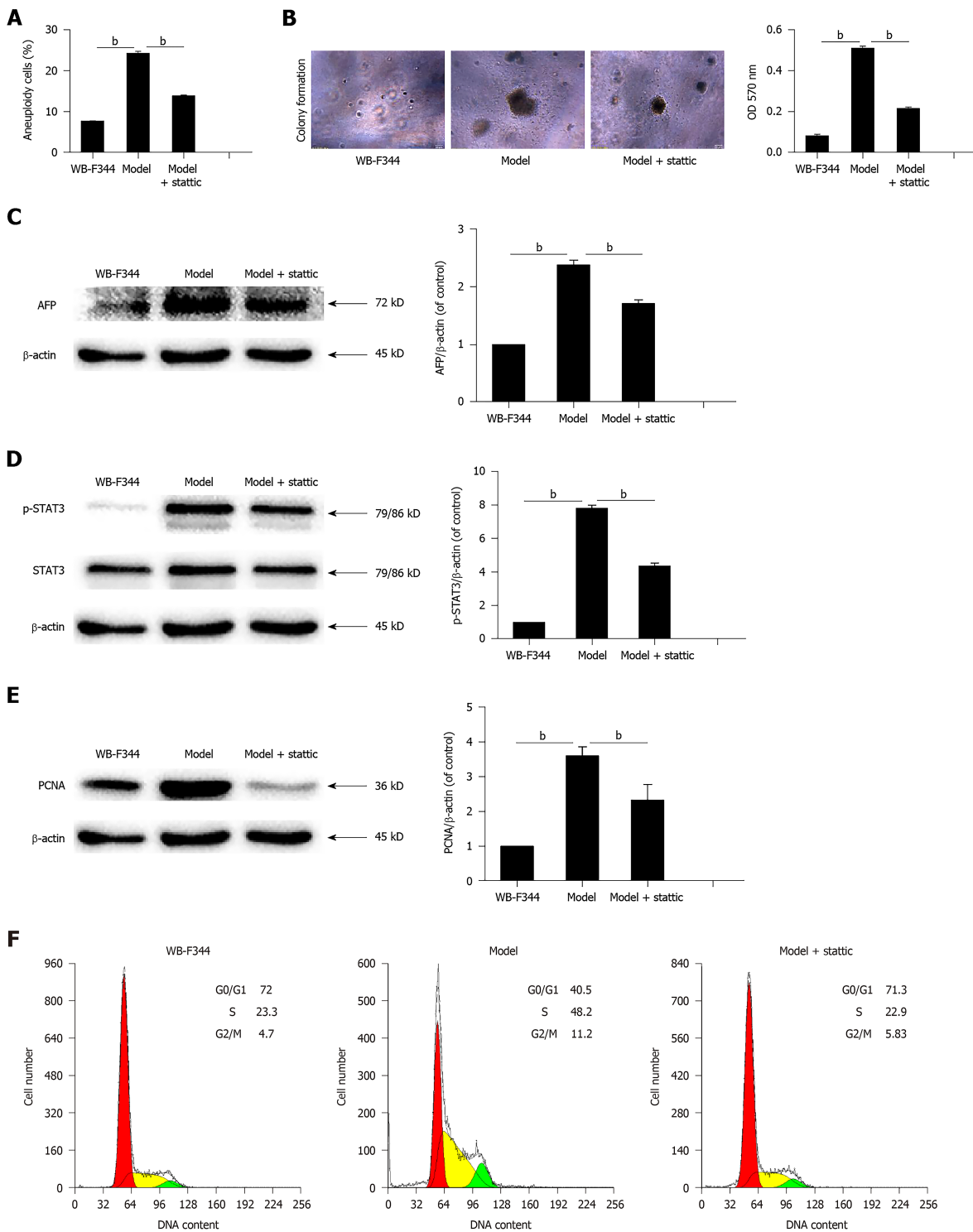


Figure 3 Activated signal transducer and activator of transcription 3 promotes malignant transformation and cell proliferation in WB-F344 cells. A-D: Aneuploidy, the soft agar colony formation rate, alpha-fetoprotein expression, and p-signal transducer and activator of transcription 3 expression in transformed WB-F344 cells induced with N-methyl-N'-nitro-N-nitroso-guanidine (MNNG) + hydrogen peroxide (H₂O₂) were increased compared with those in control WB-F344 cells and decreased following static treatment. E-G: Proliferating cell nuclear antigen expression and the percentage of cells in S phase in transformed WB-F344 cells induced with MNNG + H₂O₂ were higher than those in control WB-F344 cells and decreased following static treatment. Data are expressed as the mean ± SEM (^a*P* < 0.05, ^b*P* < 0.01). (static: 4 μmol/L, 48 h). AFP: Alpha-fetoprotein; STAT3: Signal transducer and activator of transcription 3; MNNG: N-methyl-N'-nitro-N-nitroso-guanidine; H₂O₂: Hydrogen peroxide; PCNA: Proliferating cell nuclear antigen.

differentiation of liver stem cells are two widely accepted hypotheses about the origin of liver cancer. The carcinoma might originate from mature liver cells or progenitor cells. Molecular studies have identified that adult hepatocytes are the source of HCC because they can directly degenerate into HCC following sequential genomic alterations. Alternatively, hepatic progenitor cells might generate HCC and intrahepatic cholangiocarcinoma with markers of progenitor cells^[35], because

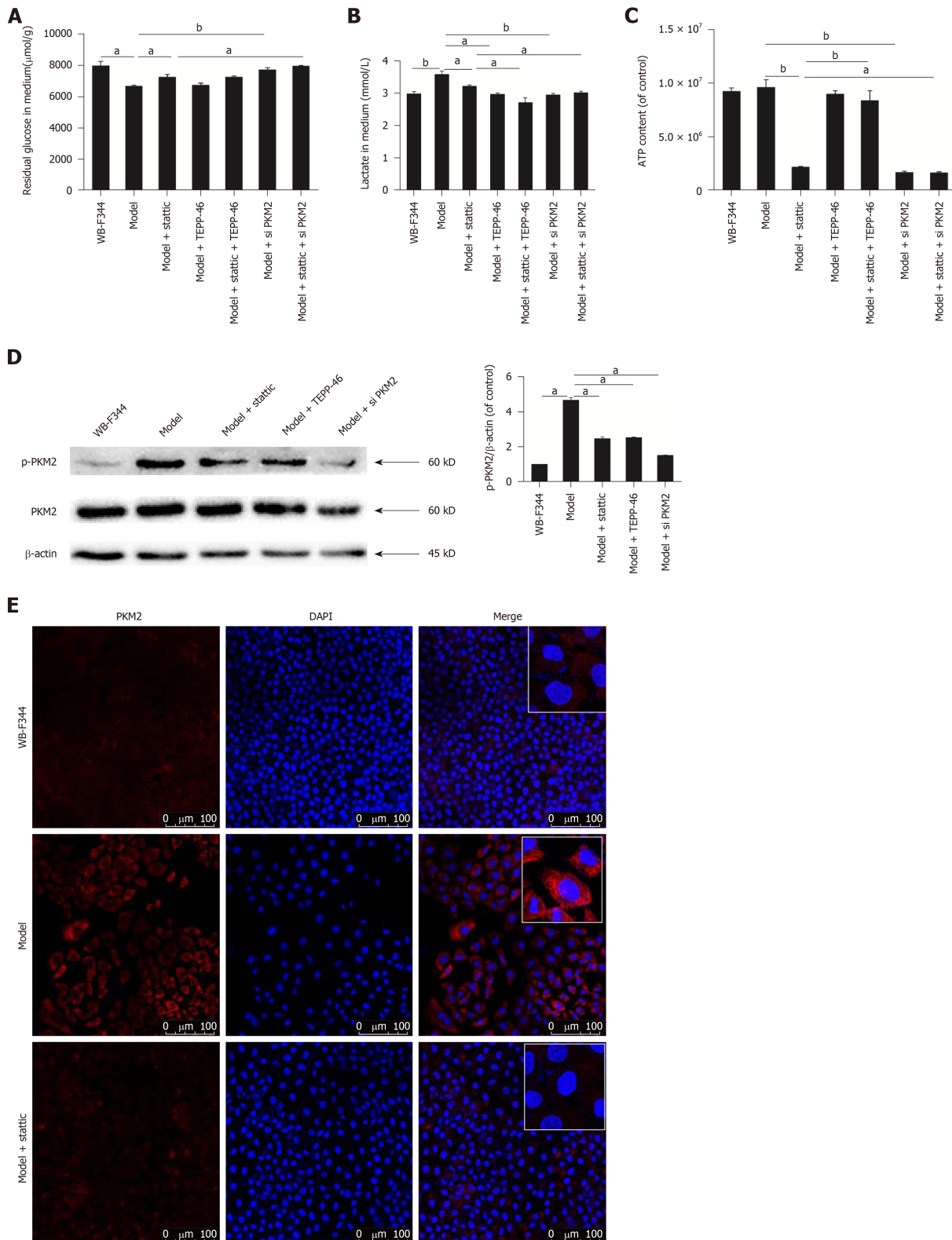


Figure 4 Activated signal transducer and activator of transcription 3 promotes the Warburg effect by enhancing p-pyruvate kinase M2 in transformed WB-F344 cells. A-C: The glucose concentration in medium in transformed WB-F344 cells induced with N-methyl-N'-nitro-N-nitroso-guanidine (MNNG) + hydrogen peroxide (H₂O₂) was lower than that in control WB-F344 cells. The lactate concentration in medium in transformed WB-F344 cells induced with MNNG + H₂O₂ was higher than that in control WB-F344 cells. Inhibition of p-signal transducer and activator of transcription 3 resulted in suppression of glucose consumption, lactate production, and ATP level. TEPP-46 and pyruvate kinase M2 (PKM2) siRNA further reduced the Warburg effect. D: The activation of p-PKM2 was elevated in transformed WB-F344 cells induced with MNNG + H₂O₂, and was inhibited following static treatment. Static, TEPP-46, and PKM2 siRNA inhibited the expression of p-PKM2 in transformed WB-F344 cells induced with MNNG + H₂O₂. E: The expression and nuclear translocation of PKM2 were elevated in transformed WB-F344 cells induced with MNNG + H₂O₂ and were inhibited following static treatment. (^aP < 0.05, ^bP < 0.01) (static: 4 μmol/L, 48 h; TEPP-46: 25 μmol/L, 24 h). MNNG: N-methyl-N'-nitro-N-nitroso-guanidine; H₂O₂: Hydrogen peroxide; STAT3: Signal transducer and activator of transcription 3; PKM2: Pyruvate kinase M2.

hepatocytes and cholangiocytes each arise from a common progenitor (hepatoblasts)

during liver development. Studies have noted a progenitor cell phenotype in many HCCs^[36]. And liver cancers with stem cell features have more aggressive clinical behavior and a worse prognosis than those without stem cell features. The Solt-Farber model is an established hepatic precancerous animal model. GST- π detoxifies electrophiles through conjugation to thiol-reduced glutathione (GSH) and is overexpressed in the early stages of carcinogenesis, including hepatic precancerous lesions. Our results confirmed that many heterocellular clusters were present in the liver parenchyma and portal area and that GST- π was highly expressed in liver precancerous lesions in Solt-Farber model rats (Figure 1C). In addition, our results revealed that OV6, a marker of hepatic progenitor cells in rats, was strongly expressed in the heterocellular clusters of the liver in the model group. As another marker of liver progenitor cells, the expression of CK19 was also elevated in the model group, suggesting that hepatic progenitor cells were activated (Figure 1D and F).

STAT3 is activated in HCC, but its effects in hepatic progenitor cells are not entirely clear. Our results revealed that p-STAT3 was strongly expressed in activated hepatic progenitor cells in the model group (Figure 1D and E), suggesting that STAT3 activation is involved in the stimulation of hepatic progenitor cells in the progression of liver precancerous lesions.

In a previous study, PKM2 promoted the Warburg effect in HCC, which provides the tumor with many advantages for cell growth and survival^[37]. However, the mechanism of PKM2 in the Warburg effect in HCC and liver precancerous lesions remains poorly understood. Our results indicate that the Warburg effect is initiated at the stage of liver precancerous lesions in rats (Figure 2A and B) and enhanced probably by PKM2 in activated hepatic progenitor cells (Figure 2C-E).

To further explore the mechanism of STAT3 in liver precancerous lesions in rats, we observed the effect of STAT3 in transformed WB-F344 cells induced with MNNG + H₂O₂. Increased aneuploidy and anchorage-independent growth are vital features of tumor cells^[38]. The size and shape of transformed WB-F344 cells changed, contact inhibition vanished, and aneuploidy, clonal formation rate, and AFP expression increased (Figure 3A-C), indicating that hepatic progenitor cells were transformed extensively. The transformed WB-F344 cells were treated with stattic, which inhibited the activation of STAT3, to observe the function of STAT3 during the malignant transformation of hepatic progenitor cells. The results showed that clonal formation rate, AFP expression, and aneuploidy fell significantly (Figure 3A-C), suggesting that STAT3 promotes malignant transformation of hepatic progenitor cells in rats. Intracellular STAT3 activation is closely associated with the cell cycle and proliferation in HCC cells. Our results also showed that STAT3 enhances malignant transformation of hepatic progenitor cells by promoting the expression of PCNA and accelerating G1/S phase transition (Figure 3E and F).

Dimeric PKM2 promotes cell proliferation and the Warburg effect in HCC^[22], but its effects in hepatic progenitor cells are still unknown. Our results show that the Warburg effect was initiated and the p-PKM2 expression and nuclear translocation were increased in transformed WB-F344 cells (Figure 4A-E). This result implies that p-PKM2 probably promotes the Warburg effect in transformed WB-F344 cells. In addition, in the Solt-Farber model, the total protein expression of PKM2 in the liver was also higher, which may be due to the complexity of the internal environment in rats compared with that in cell culture. Following stattic treatment, p-PKM2 expression and nuclear translocation decreased, and the Warburg effect was suppressed (Figure 4A-E). Further use of PKM2 siRNA on the basis of stattic treatment in transformed WB-F344 cells further reduced the Warburg effect (Figure 4A-C). An interesting result is that, treatment with TEPP-46, a potent and selective activator of PKM2, in transformed WB-F344 cells after treatment with stattic, further reduced the production of lactate, increased ATP level, but had no significant impact on glucose consumption, which is consistent with previous studies^[39,40]. The reasons are that TEPP-46 promotes the formation of PKM2 tetramer and forms an enzyme with high pyruvate kinase activity as well as mediates the last step of glycolysis by promoting glycolysis flux, and then inhibits the formation of PKM2 dimer. That is to say, TEPP-46 in fact inhibits the Warburg effect. These results indicate that STAT3 promotes the Warburg effect possibly by enhancing p-PKM2 expression in transformed hepatic progenitor cells in rats. Previous studies have demonstrated that PKM2 promoted oncogenesis probably by phosphorylating STAT3^[41]. Hence, whether there is positive feedback between STAT3 and PKM2 in malignant transformation of hepatic progenitor cells remains to be further studied.

In summary, our results provide the evidence that the Warburg effect has been initiated at the stage of the liver precancerous lesions in rats, perhaps through high expression of PKM2 and p-STAT3 in activated hepatic progenitor cells in rats. Furthermore, STAT3 promotes the Warburg effect possibly by upregulating p-PKM2 expression and leading to malignant transformation of hepatic progenitor cells in rats.

These results can help better understand the role of PKM2 and STAT3 in the formation of HCC.

ARTICLE HIGHLIGHTS

Research background

Hepatocellular carcinoma (HCC) is the fifth common malignant tumor worldwide and has a poor prognosis. HCC is closely associated with the potential precancerous lesions. Early treatment at the precancerous stage could significantly prevent the occurrence of HCC. Signal transducer and activator of transcription 3 (STAT3) and pyruvate kinase M2 (PKM2) can be activated and enhance the Warburg effect in HCC. However, whether activation of STAT3 enhances the Warburg effect in liver precancerous lesions in rats, and the relationship between STAT3 and PKM2 remain unclear. Hence, clarifying the mechanism of liver precancerous lesion of HCC are very important.

Research motivation

Investigating the mechanism of STAT3 and the Warburg effect in liver precancerous lesions in rats may suggest potential molecular mechanisms of hepatocellular carcinogenesis, and further offer the potential for developing novel therapeutic strategies for HCC treatment.

Research objectives

To measure the expression of STAT3 and PKM2, and the Warburg effect in liver precancerous lesions in rats and in transformed WB-F344 cells, and to investigate the possible molecular mechanisms of STAT3 in liver precancerous lesions.

Research methods

The Solt-Farber model is an established hepatic precancerous animal model. The transformed WB-F344 cells were induced with N-methyl-N'-nitro-N-nitrosoguanidine (MNNG) and hydrogen peroxide (H₂O₂). The contents of glucose and lactate in the tissue and culture medium of the cells were detected with a spectrophotometer. The protein levels were examined by Western blot and immunofluorescence.

Research results

Here, we provide the evidence that the Warburg effect was enhanced in liver precancerous lesions in rats, perhaps through high expression of PKM2 and p-STAT3 in activated oval cells. STAT3 activation promotes the Warburg effect by activating PKM2 in transformed WB-F344 cells induced with MNNG and H₂O₂.

Research conclusions

STAT3 activation promotes the Warburg effect by enhancing the phosphorylation of PKM2 in transformed WB-F344 cells. The Warburg effect, PKM2 and STAT3 expression were increased in liver precancerous lesions in rats.

Research perspectives

We have carried out some rat experiments and *in vitro* cell experiments, but further studies are needed to explore the mechanism of liver precancerous lesions. We also need to collect clinical samples for further validation. STAT3 and PKM2 may be potential diagnostic or therapeutic targets and used for clinical diagnosis and therapy in the future.

REFERENCES

- 1 **Beyoğlu D**, Imbeaud S, Maurhofer O, Bioulac-Sage P, Zucman-Rossi J, Dufour JF, Idle JR. Tissue metabolomics of hepatocellular carcinoma: tumor energy metabolism and the role of transcriptomic classification. *Hepatology* 2013; **58**: 229-238 [PMID: 23463346 DOI: 10.1002/hep.26350]
- 2 **Sun L**, Suo C, Li ST, Zhang H, Gao P. Metabolic reprogramming for cancer cells and their microenvironment: Beyond the Warburg Effect. *Biochim Biophys Acta Rev Cancer* 2018; **1870**: 51-66 [PMID: 29959989 DOI: 10.1016/j.bbcan.2018.06.005]
- 3 **Song P**, Cai Y, Tang H, Li C, Huang J. The clinical management of hepatocellular carcinoma worldwide: A concise review and comparison of current guidelines from 2001 to 2017. *Biosci Trends* 2017; **11**: 389-398 [PMID: 28904327 DOI: 10.5582/bst.2017.01202]
- 4 **Muramatsu S**, Tanaka S, Mogushi K, Adikrisna R, Aihara A, Ban D, Ochiai T, Irie T, Kudo A, Nakamura N, Nakayama K, Tanaka H, Yamaoka S, Arii S. Visualization of stem cell features in human hepatocellular carcinoma reveals *in vivo* significance of tumor-host interaction and clinical course. *Hepatology* 2013; **58**: 218-228 [PMID: 23447025 DOI: 10.1002/hep.26345]
- 5 **Yang Y**, Lin X, Lu X, Luo G, Zeng T, Tang J, Jiang F, Li L, Cui X, Huang W, Hou G, Chen X, Ouyang Q, Tang S, Sun H, Chen L, Gonzalez FJ, Wu M, Cong W, Chen L, Wang H. Interferon-microRNA signalling drives liver precancerous lesion formation and hepatocarcinogenesis. *Gut* 2016; **65**: 1186-1201 [PMID: 26860770 DOI: 10.1136/gutjnl-2015-310318]
- 6 **Mishra L**, Banker T, Murray J, Byers S, Thenappan A, He AR, Shetty K, Johnson L, Reddy EP. Liver stem cells and hepatocellular carcinoma. *Hepatology* 2009; **49**: 318-329 [PMID: 19111019 DOI: 10.1002/hep.22704]
- 7 **Sell S**. On the stem cell origin of cancer. *Am J Pathol* 2010; **176**: 2584-2494 [PMID: 20431026 DOI: 10.1053/j.ajcp.2010.05.005]

- 10.2353/ajpath.2010.091064]
- 8 **Sangan CB**, Tosh D. Hepatic progenitor cells. *Cell Tissue Res* 2010; **342**: 131-137 [PMID: 20957497 DOI: 10.1007/s00441-010-1055-8]
 - 9 **Lu Y**, Yue X, Cui Y, Zhang J, Wang K. MicroRNA-124 suppresses growth of human hepatocellular carcinoma by targeting STAT3. *Biochem Biophys Res Commun* 2013; **441**: 873-879 [PMID: 24211205 DOI: 10.1016/j.bbrc.2013.10.157]
 - 10 **Marotta LL**, Almendro V, Marusyk A, Shipitsin M, Schemme J, Walker SR, Bloushtain-Qimron N, Kim JJ, Choudhury SA, Maruyama R, Wu Z, Gönen M, Mulvey LA, Bessarabova MO, Huh SJ, Silver SJ, Kim SY, Park SY, Lee HE, Anderson KS, Richardson AL, Nikolskaya T, Nikolsky Y, Liu XS, Root DE, Hahn WC, Frank DA, Polyak K. The JAK2/STAT3 signaling pathway is required for growth of CD44CD24 stem cell-like breast cancer cells in human tumors. *J Clin Invest* 2011; **121**: 2723-2735 [PMID: 21633165 DOI: 10.1172/JCI44745]
 - 11 **Sugimura K**, Miyata H, Tanaka K, Hamano R, Takahashi T, Kurokawa Y, Yamasaki M, Nakajima K, Takiguchi S, Mori M, Doki Y. Let-7 expression is a significant determinant of response to chemotherapy through the regulation of IL-6/STAT3 pathway in esophageal squamous cell carcinoma. *Clin Cancer Res* 2012; **18**: 5144-5153 [PMID: 22847808 DOI: 10.1158/1078-0432.CCR-12-0701]
 - 12 **Schindler C**, Levy DE, Decker T. JAK-STAT signaling: from interferons to cytokines. *J Biol Chem* 2007; **282**: 20059-20063 [PMID: 17502367 DOI: 10.1074/jbc.R700016200]
 - 13 **Yu H**, Lee H, Herrmann A, Buettner R, Jove R. Revisiting STAT3 signalling in cancer: new and unexpected biological functions. *Nat Rev Cancer* 2014; **14**: 736-746 [PMID: 25342631 DOI: 10.1038/nrc3818]
 - 14 **Jiang S**, Zhang LF, Zhang HW, Hu S, Lu MH, Liang S, Li B, Li Y, Li D, Wang ED, Liu MF. A novel miR-155/miR-143 cascade controls glycolysis by regulating hexokinase 2 in breast cancer cells. *EMBO J* 2012; **31**: 1985-1998 [PMID: 22354042 DOI: 10.1038/emboj.2012.45]
 - 15 **Qin X**, Lin L, Cao L, Zhang X, Song X, Hao J, Zhang Y, Wei R, Huang X, Lu J, Ge Q. Extracellular matrix protein Reelin promotes myeloma progression by facilitating tumor cell proliferation and glycolysis. *Sci Rep* 2017; **7**: 45305 [PMID: 28345605 DOI: 10.1038/srep45305]
 - 16 **Israelsen WJ**, Dayton TL, Davidson SM, Fiske BP, Hosios AM, Bellinger G, Li J, Yu Y, Sasaki M, Horner JW, Burga LN, Xie J, Jurezak MJ, DePinho RA, Clish CB, Jacks T, Kibbey RG, Wulf GM, Di Vizio D, Mills GB, Cantley LC, Vander Heiden MG. PKM2 isoform-specific deletion reveals a differential requirement for pyruvate kinase in tumor cells. *Cell* 2013; **155**: 397-409 [PMID: 24120138 DOI: 10.1016/j.cell.2013.09.025]
 - 17 **Sradhanjali S**, Reddy MM. Inhibition of Pyruvate Dehydrogenase Kinase as a Therapeutic Strategy against Cancer. *Curr Top Med Chem* 2018; **18**: 444-453 [PMID: 29788890 DOI: 10.2174/1568026618666180523105756]
 - 18 **Israelsen WJ**, Vander Heiden MG. Pyruvate kinase: Function, regulation and role in cancer. *Semin Cell Dev Biol* 2015; **43**: 43-51 [PMID: 26277545 DOI: 10.1016/j.semcdb.2015.08.004]
 - 19 **Morita M**, Sato T, Nomura M, Sakamoto Y, Inoue Y, Tanaka R, Ito S, Kurosawa K, Yamaguchi K, Sugiura Y, Takizaki H, Yamashita Y, Katakura R, Sato I, Kawai M, Okada Y, Watanabe H, Kondoh G, Matsumoto S, Kishimoto A, Obata M, Matsumoto M, Fukuhara T, Motohashi H, Suematsu M, Komatsu M, Nakayama KI, Watanabe T, Soga T, Shima H, Maemondo M, Tanuma N. PKM1 Confers Metabolic Advantages and Promotes Cell-Autonomous Tumor Cell Growth. *Cancer Cell* 2018; **33**: 355-367.e7 [PMID: 29533781 DOI: 10.1016/j.ccell.2018.02.004]
 - 20 **Yang W**, Lu Z. Pyruvate kinase M2 at a glance. *J Cell Sci* 2015; **128**: 1655-1660 [PMID: 25770102 DOI: 10.1242/jcs.166629]
 - 21 **Christofk HR**, Vander Heiden MG, Wu N, Asara JM, Cantley LC. Pyruvate kinase M2 is a phosphotyrosine-binding protein. *Nature* 2008; **452**: 181-186 [PMID: 18337815 DOI: 10.1038/nature06667]
 - 22 **Iansante V**, Choy PM, Fung SW, Liu Y, Chai JG, Dyson J, Del Rio A, D'Santos C, Williams R, Chokshi S, Anders RA, Bubici C, Papa S. PARP14 promotes the Warburg effect in hepatocellular carcinoma by inhibiting JNK1-dependent PKM2 phosphorylation and activation. *Nat Commun* 2015; **6**: 7882 [PMID: 26258887 DOI: 10.1038/ncomms8882]
 - 23 **Solt DB**, Medline A, Farber E. Rapid emergence of carcinogen-induced hyperplastic lesions in a new model for the sequential analysis of liver carcinogenesis. *Am J Pathol* 1977; **88**: 595-618 [PMID: 18937]
 - 24 **Luo Q**, Siconolfi-Baez L, Annamaneni P, Bielawski MT, Novikoff PM, Angeletti RH. Altered protein expression at early-stage rat hepatic neoplasia. *Am J Physiol Gastrointest Liver Physiol* 2007; **292**: G1272-G1282 [PMID: 17272515 DOI: 10.1152/ajpgi.00474.2006]
 - 25 **Han YY**, Xue XW, Shi ZM, Wang PY, Wu XR, Wang XJ. Oleonic acid and ursolic acid inhibit proliferation in transformed rat hepatic oval cells. *World J Gastroenterol* 2014; **20**: 1348-1356 [PMID: 24574810 DOI: 10.3748/wjg.v20.i5.1348]
 - 26 **Ding L**, Ding YN, Lin Y, Wen JM, Xue L. Proteins related to early changes in carcinogenesis of hepatic oval cells after treatment with methylnitrosoguanidine. *Exp Toxicol Pathol* 2014; **66**: 139-146 [PMID: 24360059 DOI: 10.1016/j.etp.2013.11.007]
 - 27 **Ganem NJ**, Storchova Z, Pellman D. Tetraploidy, aneuploidy and cancer. *Curr Opin Genet Dev* 2007; **17**: 157-162 [PMID: 17324569 DOI: 10.1016/j.gde.2007.02.011]
 - 28 **Soma Y**, Satoh K, Sato K. Purification and subunit-structural and immunological characterization of five glutathione S-transferases in human liver, and the acidic form as a hepatic tumor marker. *Biochim Biophys Acta* 1986; **869**: 247-258 [PMID: 2418879]
 - 29 **Dunsford HA**, Karnasuta C, Hunt JM, Sell S. Different lineages of chemically induced hepatocellular carcinoma in rats defined by monoclonal antibodies. *Cancer Res* 1989; **49**: 4894-4900 [PMID: 2474377]
 - 30 **Li XF**, Chen C, Xiang DM, Qu L, Sun W, Lu XY, Zhou TF, Chen SZ, Ning BF, Cheng Z, Xia MY, Shen WF, Yang W, Wen W, Lee TKW, Cong WM, Wang HY, Ding J. Chronic inflammation-elicited liver progenitor cell conversion to liver cancer stem cell with clinical significance. *Hepatology* 2017; **66**: 1934-1951 [PMID: 28714104 DOI: 10.1002/hep.29372]
 - 31 **Christofk HR**, Vander Heiden MG, Harris MH, Ramanathan A, Gerszten RE, Wei R, Fleming MD, Schreiber SL, Cantley LC. The M2 splice isoform of pyruvate kinase is important for cancer metabolism and tumour growth. *Nature* 2008; **452**: 230-233 [PMID: 18337823 DOI: 10.1038/nature06734]
 - 32 **Ferguson EC**, Rathmell JC. New roles for pyruvate kinase M2: working out the Warburg effect. *Trends Biochem Sci* 2008; **33**: 359-362 [PMID: 18603432 DOI: 10.1016/j.tibs.2008.05.006]
 - 33 **Palsson-McDermott EM**, Curtis AM, Goel G, Lauterbach MAR, Sheedy FJ, Gleeson LE, van den Bosch MWM, Quinn SR, Domingo-Fernandez R, Johnston DGW, Jiang JK, Israelsen WJ, Keane J, Thomas C,

- Clish C, Vander Heiden M, Xavier RJ, O'Neill LAJ. Pyruvate Kinase M2 Regulates Hif-1 α Activity and IL-1 β Induction and Is a Critical Determinant of the Warburg Effect in LPS-Activated Macrophages. *Cell Metab* 2015; **21**: 347 [PMID: 29510100 DOI: 10.1016/j.cmet.2015.01.017]
- 34 **Darnell JE.** STAT3, HIF-1, glucose addiction and Warburg effect. *Aging (Albany NY)* 2010; **2**: 890-891 [PMID: 21149895 DOI: 10.18632/aging.100239]
- 35 **Sia D,** Villanueva A, Friedman SL, Llovet JM. Liver Cancer Cell of Origin, Molecular Class, and Effects on Patient Prognosis. *Gastroenterology* 2017; **152**: 745-761 [PMID: 28043904 DOI: 10.1053/j.gastro.2016.11.048]
- 36 **Qiu L,** Li H, Fu S, Chen X, Lu L. Surface markers of liver cancer stem cells and innovative targeted-therapy strategies for HCC. *Oncol Lett* 2018; **15**: 2039-2048 [PMID: 29434903 DOI: 10.3892/ol.2017.7568]
- 37 **Xu Q,** Tu J, Dou C, Zhang J, Yang L, Liu X, Lei K, Liu Z, Wang Y, Li L, Bao H, Wang J, Tu K. HSP90 promotes cell glycolysis, proliferation and inhibits apoptosis by regulating PKM2 abundance via Thr-328 phosphorylation in hepatocellular carcinoma. *Mol Cancer* 2017; **16**: 178 [PMID: 29262861 DOI: 10.1186/s12943-017-0748-y]
- 38 **Fang X,** Zhang P. Aneuploidy and tumorigenesis. *Semin Cell Dev Biol* 2011; **22**: 595-601 [PMID: 21392584 DOI: 10.1016/j.semcdb.2011.03.002]
- 39 **Anastasiou D,** Yu Y, Israelsen WJ, Jiang JK, Boxer MB, Hong BS, Tempel W, Dimov S, Shen M, Jha A, Yang H, Mattaini KR, Metallo CM, Fiske BP, Courtney KD, Malstrom S, Khan TM, Kung C, Skoumbourdis AP, Veith H, Southall N, Walsh MJ, Brimacombe KR, Leister W, Lunt SY, Johnson ZR, Yen KE, Kunii K, Davidson SM, Christofk HR, Austin CP, Inglesse J, Harris MH, Asara JM, Stephanopoulos G, Salituro FG, Jin S, Dang L, Auld DS, Park HW, Cantley LC, Thomas CJ, Vander Heiden MG. Pyruvate kinase M2 activators promote tetramer formation and suppress tumorigenesis. *Nat Chem Biol* 2012; **8**: 839-847 [PMID: 22922757 DOI: 10.1038/nchembio.1060]
- 40 **Nakatsu D,** Horiuchi Y, Kano F, Noguchi Y, Sugawara T, Takamoto I, Kubota N, Kadowaki T, Murata M. L-cysteine reversibly inhibits glucose-induced biphasic insulin secretion and ATP production by inactivating PKM2. *Proc Natl Acad Sci USA* 2015; **112**: E1067-E1076 [PMID: 25713368 DOI: 10.1073/pnas.1417197112]
- 41 **Tamada M,** Suematsu M, Saya H. Pyruvate kinase M2: multiple faces for conferring benefits on cancer cells. *Clin Cancer Res* 2012; **18**: 5554-5561 [PMID: 23071357 DOI: 10.1158/1078-0432.CCR-12-0859]



Published By Baishideng Publishing Group Inc
7041 Koll Center Parkway, Suite 160, Pleasanton, CA 94566, USA
Telephone: +1-925-2238242
Fax: +1-925-2238243
E-mail: bpgoffice@wjgnet.com
Help Desk: <http://www.f6publishing.com/helpdesk>
<http://www.wjgnet.com>

